Quantized Conductance at the Majorana Phase Transition in a Disordered Superconducting Wire

Akhmerov, A.R.; Dahlhaus, J.P.; Hassler, F.; Wimmer, M.; Beenakker, C.W.J.

Quantized Conductance at the Majorana Phase Transition in a Disordered Superconducting Wire

A. R. Akhmerov, J. P. Dahlhaus, F. Hassler, M. Wimmer, and C. W. J. Beenakker
Instituut-Lorentz, Universiteit Leiden, Post Office Box 9506, 2300 RA Leiden, The Netherlands
(Received 28 September 2010; published 31 January 2011)

Superconducting wires without time-reversal and spin-rotation symmetries can be driven into a topological phase that supports Majorana bound states. Direct detection of these zero-energy states is complicated by the proliferation of low-lying excitations in a disordered multimode wire. We show that the phase transition itself is signaled by a quantized thermal conductance and electrical shot noise power, irrespective of the degree of disorder. In a ring geometry, the phase transition is signaled by a period doubling of the magnetoconductance oscillations. These signatures directly follow from the identification of the sign of the determinant of the reflection matrix as a topological quantum number.

DOI: 10.1103/PhysRevLett.106.057001 PACS numbers: 74.78.Na, 03.65.Vf, 74.25.fc, 74.45.+c

It has been predicted theoretically [1] that the *s*-wave proximity effect of a superconducting substrate can drive a spin-polarized and spin-orbit coupled semiconductor nanowire into a topological phase [2–4], with a Majorana fermion trapped at each end of the wire. There exists now a variety of proposals [5–7] for topological quantum computing in nanowires that hope to benefit from the long coherence time expected for Majorana fermions. A superconducting proximity effect in InAs wires (which have the required strong spin-orbit coupling) has already been demonstrated in zero magnetic field [8], and now the experimental challenge is to drive the system through the Majorana phase transition in a parallel field.

Proposals to detect the topological phase have focused on the detection of the Majorana bound states at the end points of the wire, through their effect on the current-voltage characteristic [9,10] or the ac Josephson effect [11,12]. These signatures of the topological phase would stand out in a clean single-mode wire, but the multiple modes and potential fluctuations in a realistic system are expected to produce a chain of coupled Majorana's [13,14], which would form a band of low-lying excitations that would be difficult to distinguish from ordinary fermionic bound states [15].

Here we propose an altogether different detection strategy: Rather than trying to detect the Majorana bound states inside the topological phase, we propose to detect the phase transition itself. A topological phase transition is characterized by a change in the topological quantum number Q. The value of $Q = (-1)^m$ is determined by the parity of the number m of Majorana bound states at each end of the wire, with $Q = -1$ in the topological phase [16].

In accord with earlier work [17], we relate the topological quantum number to the determinant of the matrix r of quasiparticle reflection amplitudes, which crosses zero at the phase transition. This immediately implies a unit transmission eigenvalue at the transition. Disorder may shift the position of the transition but it cannot affect the unit height of the transmission peak. We propose experiments to measure the transmission peak in both thermal and electrical transport properties, and support our analytical predictions by computer simulations.

We consider a two-terminal transport geometry, consisting of a disordered superconducting wire of length L, connected by clean normal-metal leads to reservoirs in thermal equilibrium (temperature τ_0). The leads support $2N$ right-moving modes and $2N$ left-moving modes at the Fermi level, with mode amplitudes ψ_+ and ψ_-, respectively. The spin degree of freedom is included in the number N, while the factor of 2 counts the electron and hole degree of freedom.

The $4N \times 4N$ unitary scattering matrix $\mathcal{S}$ relates incoming and outgoing mode amplitudes,

$$\begin{pmatrix} \psi_{-,L} \\ \psi_{+,R} \end{pmatrix} = \mathcal{S} \begin{pmatrix} \psi_{+,L} \\ \psi_{-,R} \end{pmatrix}, \qquad \mathcal{S} = \begin{pmatrix} r & t' \\ t & r' \end{pmatrix}, \tag{1}$$

where the labels L and R distinguish modes in the left and right lead. The four blocks of $\mathcal{S}$ define the $2N \times 2N$ reflection matrices r, r' and transmission matrices t, t'.

Time-reversal symmetry and spin-rotation symmetry are broken in the superconductor, but electron-hole symmetry remains. At the Fermi energy electron-hole symmetry implies that if (u, v) is an electron-hole eigenstate, then also (v^*, u^*). Using this symmetry we can choose a basis such that all modes have purely real amplitudes. In this socalled Majorana basis $\mathcal{S}$ is a real orthogonal matrix, $\mathcal{S}^{\mathrm{t}} = \mathcal{S}^\dagger = \mathcal{S}^{-1}$. (The superscript t indicates the transpose of a matrix.) More specifically, since $\det \mathcal{S} = 1$ the scattering matrix is an element of the special orthogonal group SO($4N$). This is symmetry class D [18–23].

The scattering matrix in class D has the polar decomposition

$$\mathcal{S} = \begin{pmatrix} O_1 & 0 \\ 0 & O_2 \end{pmatrix} \begin{pmatrix} \tanh\Lambda & (\cosh\Lambda)^{-1} \\ (\cosh\Lambda)^{-1} & -\tanh\Lambda \end{pmatrix} \begin{pmatrix} O_3 & 0 \\ 0 & O_4 \end{pmatrix}, \tag{2}$$

in terms of four orthogonal matrices $O_p \in \mathrm{SO}(2N)$ and a diagonal real matrix Λ with diagonal elements $\lambda_n \in (-\infty, \infty)$. The absolute value $|\lambda_n|$ is called a Lyapunov exponent, related to the transmission eigenvalue $T_n \in [0, 1]$ by $T_n = 1/\cosh^2\lambda_n$. We identify

$$Q = \mathrm{sign}\,\mathcal{Q}, \qquad \mathcal{Q} = \mathrm{Det}r = \mathrm{Det}r' = \prod_{n=1}^{2N} \tanh\lambda_n. \quad (3)$$

This relation expresses the fact that reflection from a Majorana bound state contributes a scattering phase shift of π, so a phase factor of -1. The sign of $\prod_n \tanh\lambda_n$ thus equals the parity of the number m of Majorana bound states at one end of the wire [24]. (It makes no difference which end, and indeed r and r' give the same Q.)

To put this expression for Q into context, we first note that it may be written equivalently as $Q = \mathrm{Det}O_1O_3$ if we restrict the λ_n's to non-negative values and allow $\mathrm{Det}O_p$ to equal either $+1$ or -1. The sign of Q then corresponds to the topological classification of a class-D network model derived by Merz and Chalker [17]. We also note that Q can be written equivalently in terms of the Pfaffian of $\ln\mathcal{M}\mathcal{M}^\dagger$ (with $\mathcal{M}$ the transfer matrix in a suitable basis) [24]. A Pfaffian relation for the topological quantum number Q_{clean} in class D has been derived by Kitaev [4] for a clean, translationally invariant system. We will verify later on that Q and Q_{clean} agree for a clean system.

An immediate consequence of Eq. (3) is that at the topological phase transition one of the λ_n's vanishes [17,20,21], so the corresponding transmission eigenvalue $T_n = 1$ at the transition point. The sign change of Q ensures that T_n fully reaches its maximal value of unity, it cannot stop short of it without introducing a discontinuity in $\mathcal{Q}$. Generically, there will be only a single unit transmission eigenvalue at the transition, the others being exponentially suppressed by the superconducting gap. The thermal conductance $G_{\mathrm{th}} = G_0\sum_n T_n$ of the wire will then show a peak of quantized height $G_0 = \pi^2 k_B^2\tau_0/6h$ at the transition.

Our claim of a quantized conductance at the transition point is consistent with earlier work [19–22] on class D ensembles. There a broad distribution of the conductance was found in the large-L limit, but the key difference is that we are considering a single disordered sample of finite length, and the value of the control parameter at which the conductance is quantized is sample specific. We will now demonstrate how the peak of quantized conductance arises, first for a simple analytically solvable model, then for a more complete microscopic Hamiltonian that we solve numerically.

The analytically solvable model is the effective low-energy Hamiltonian of a class-D superconductor with a random gap, which for a single mode in the Majorana basis has the form

$$H = -i\hbar v_F\sigma_z\partial/\partial x + \Delta(x)\sigma_y. \quad (4)$$

We have assumed, for simplicity, that right-movers and left-movers have the same velocity v_F, but otherwise this is the generic form to linear order in momentum, constrained by the electron-hole symmetry requirement $H = -H^*$. An eigenstate Ψ of H at energy zero satisfies

$$\Psi(x) = \exp\left(-\frac{1}{\hbar v_F}\sigma_x\int_0^x \Delta(x')dx'\right)\Psi(0). \quad (5)$$

By substituting $\Psi(0) = (1, r)$, $\Psi(L) = (t, 0)$ we obtain the reflection amplitude

$$r = \tanh(L\bar{\Delta}/\hbar v_F), \qquad \bar{\Delta} = L^{-1}\int_0^L \Delta(x)dx. \quad (6)$$

In this simple model, a change of sign of the spatially averaged gap $\bar{\Delta}$ is the signature of a topological phase transition [25].

If $\bar{\Delta}$ is varied by some external control parameter, the thermal conductance $G_{\mathrm{th}} = G_0\cosh^{-2}(L\bar{\Delta}/\hbar v_F)$ has a peak at the transition point $\bar{\Delta} = 0$, of height G_0 and width $\hbar v_F/L$ (Thouless energy). The $1/\cosh^2$ line shape is the same as for a thermally broadened tunneling resonance, but the quantized peak height (irrespective of any asymmetry in the coupling to the left and right lead) is highly distinctive.

For a more realistic microscopic description of the quantized conductance peak, we have performed a numerical simulation of the model [1] of a semiconductor nanowire on a superconducting substrate. The Bogoliubov–de Gennes Hamiltonian

$$\mathcal{H} = \begin{pmatrix} H_R - E_F & \Delta \\ \Delta^* & E_F - \sigma_y H_R^*\sigma_y \end{pmatrix} \quad (7)$$

couples electron and hole excitations near the Fermi energy E_F through an s-wave superconducting order parameter Δ. Electron-hole symmetry is expressed by

$$\sigma_y\tau_y\mathcal{H}^*\sigma_y\tau_y = -\mathcal{H}, \quad (8)$$

where the Pauli matrices σ_y and τ_y act, respectively, on the spin and the electron-hole degree of freedom. The excitations are confined to a wire of width W and length L in the x-y plane of the semiconductor surface inversion layer, where their dynamics is governed by the Rashba Hamiltonian

$$H_R = \frac{\boldsymbol{p}^2}{2m_{\mathrm{eff}}} + U(\boldsymbol{r}) + \frac{\alpha_{\mathrm{so}}}{\hbar}(\sigma_x p_y - \sigma_y p_x) + \frac{1}{2}g_{\mathrm{eff}}\mu_B B\sigma_x. \quad (9)$$

The spin is coupled to the momentum $\boldsymbol{p} = -i\hbar\partial/\partial\boldsymbol{r}$ by the Rashba effect, and polarized through the Zeeman effect by a magnetic field B parallel to the wire (in the x direction). Characteristic length and energy scales are $l_{\mathrm{so}} = \hbar^2/m_{\mathrm{eff}}\alpha_{\mathrm{so}}$ and $E_{\mathrm{so}} = m_{\mathrm{eff}}\alpha_{\mathrm{so}}^2/\hbar^2$. Typical values in InAs are $l_{\mathrm{so}} = 100$ nm, $E_{\mathrm{so}} = 0.1$ meV, $g_{\mathrm{eff}}\mu_B = 2$ meV/T.

We have solved the scattering problem numerically [26] by discretizing the Hamiltonian (7) on a square lattice (lattice constant a), with a short-range electrostatic disorder potential $U(x, y)$ that varies randomly from site to site, distributed uniformly in the interval $(-U_0, U_0)$.

(Equivalent results are obtained for long-range disorder [24].) The disordered superconducting wire (S) is connected at the two ends to clean metal leads (N_1, N_2), obtained by setting $U \equiv 0$, $\Delta \equiv 0$ for $x < 0$, $x > L$. Results for the thermal conductance and topological quantum number are shown in Fig. 1, as a function of the Fermi energy (corresponding to a variation in gate voltage). For the parameters listed in the caption the number N of modes in the normal leads increases from 1 to 2 at $E_F/E_{\rm so} \approx 10$ and from 2 to 3 at $E_F/E_{\rm so} \approx 15$. We emphasize that Fig. 1 shows raw data, without any averaging over disorder.

For a clean system ($U_0 = 0$, black curves) the results are entirely as expected: A topologically nontrivial phase (with Det$r < 0$) may appear for odd N while there is no topological phase for N even [27–29]. The topological quantum number of an infinitely long clean wire (when the component p_x of momentum along the wire is a good quantum number) can be calculated from the Hamiltonian $\mathcal{H}(p_x)$ using Kitaev's Pfaffian formula [4,29],

$$Q_{\rm clean} = \mathrm{sgn}(\mathrm{Pf}[\sigma_y\tau_y H(0)]\mathrm{Pf}[\sigma_y\tau_y H(\pi/a)]). \qquad (10)$$

(The multiplication by $\sigma_y\tau_y$ ensures that the Pfaffian is calculated of an antisymmetric matrix.) The arrows in Fig. 1 indicate where $Q_{\rm clean}$ changes sign, in good agreement with the sign change of Q calculated from Eq. (3). (The agreement is not exact because L is finite.)

Upon adding disorder $Q_{\rm clean}$ can no longer be used (because p_x is no longer conserved), and we rely on a sign change of Q to locate the topological phase transition.

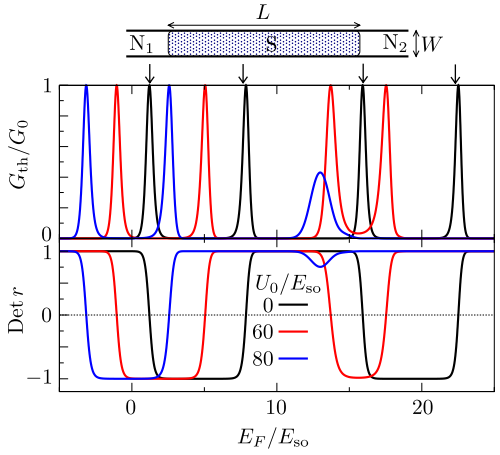

FIG. 1 (color online). Thermal conductance and determinant of reflection matrix of a disordered multimode superconducting wire as a function of Fermi energy. The curves are calculated numerically from the Hamiltonian (7)–(9) on a square lattice (lattice constant $a = l_{\rm so}/20$), for parameter values $W = l_{\rm so}$, $L = 10l_{\rm so}$, $\Delta = 10E_{\rm so}$, $g_{\rm eff}\mu_B B = 21E_{\rm so}$, and three different disorder strengths U_0. The arrows indicate the expected position of the topological phase transition in an infinite clean wire ($U_0 = 0$, $L \to \infty$), calculated from Eq. (10). Disorder reduces the topologically nontrivial interval (where Det$r < 0$), and may even remove it completely, but the conductance quantization remains unaffected as long as the phase transition persists.

Figure 1 shows that disorder moves the peaks closer together, until they merge and the topological phase disappears for sufficiently strong disorder. We have also observed the inverse process, a disorder-induced splitting of a peak and the appearance of a topological phase, in a different parameter regime than shown in Fig. 1. Our key point is that, as long as the phase transition persists, disorder has no effect on the height of the conductance peak, which remains precisely quantized—without any finite-size effects.

Since electrical conduction is somewhat easier to measure than thermal conduction, we now discuss two alternative signatures of the topological phase transition which are purely electrical. An electrical current I_1 is injected into the superconducting wire from the normal-metal contact N_1, which is at a voltage V_1 relative to the grounded superconductor. An electrical current I_2 is transmitted as quasiparticles into the grounded contact N_2, the difference $I_1 - I_2$ being drained to ground as Cooper pairs via the superconductor. The nonlocal conductance $G = \bar{I}_2/V_1$ is determined by the time averaged current $\bar{I}_2$, while the correlator of the time dependent fluctuations δI_2 determines the shot noise power $P = \int_{-\infty}^{\infty} dt \langle \delta I_2(0)\delta I_2(t)\rangle$ (in the regime $k_B\tau_0 \ll eV_1$ where thermal noise can be neglected).

These two electrical transport properties are given in terms of the $N \times N$ transmission matrices t_{ee} and t_{he} (from electron to electron and from electron to hole) by the expressions [30]

$$G = (e^2/h)\mathrm{Tr}\mathcal{T}_-, \qquad P = (e^3V_1/h)\mathrm{Tr}(\mathcal{T}_+ - \mathcal{T}_-^2), \qquad (11)$$

$$\mathcal{T}_\pm = t_{ee}^\dagger t_{ee} \pm t_{he}^\dagger t_{he}. \qquad (12)$$

Electron-hole symmetry relates $t_{ee} = t_{hh}^*$ and $t_{he} = t_{eh}^*$. This directly implies that $\mathrm{Tr}\mathcal{T}_+ = \frac{1}{2}\mathrm{Tr}tt^\dagger = \frac{1}{2}\sum_n T_n$. If in addition we assume that at most one of the T_n's is nonzero we find that $\mathcal{T}_-$ vanishes [24]. We conclude that G remains zero across the topological phase transition, while P/V_1 peaks at the quantized value $e^3/2h$. This is the second signature of the phase transition [31].

The third signature is in the electrical conductance. Since $G = 0$ for a single open transmission channel, we add (topologically trivial) open channels by means of a parallel normal-metal conductor in a ring geometry. A magnetic flux Φ through the ring produces Aharonov-Bohm oscillations with a periodicity $\Delta\Phi = h/e^*$. The effective charge $e^* = e$ if electrons or holes can be transmitted individually through the superconducting arm of the ring, while $e^* = 2e$ if only Cooper pairs can be transmitted [32,33]. We thus expect a period doubling from $h/2e$ to h/e of the magnetoconductance oscillations at the phase transition, which is indeed observed in the computer simulations (Fig. 2). To show the relative robustness of the effect to thermal averaging, we repeated the calculation at several different temperatures τ_0. For $E_{\rm so} \simeq 0.1$ meV the characteristic peak at the phase transition remains visible

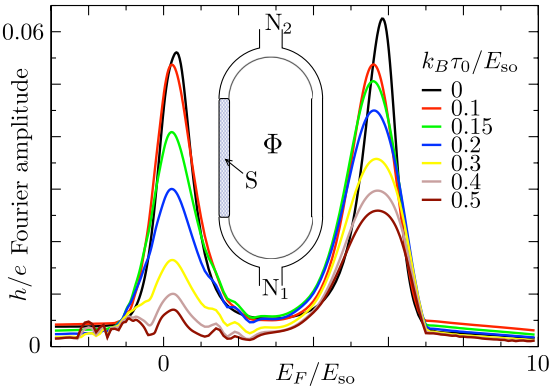

FIG. 2 (color online). Fourier amplitude with flux periodicity h/e of the magnetoconductance oscillations, calculated numerically from the Hamiltonian (7)–(9) for a single disorder strength $U_0 = 50E_{so}$ and seven different temperatures τ_0. The inset shows the Aharonov-Bohm ring geometry. The parameters of the superconducting segment of the ring (S) are the same as in Fig. 1, with $N = 1$ in this range of Fermi energies. The normal part of the ring has $N = 8$ propagating modes to avoid localization by the disorder (which has the same strength throughout the ring).

for temperatures in the readily accessible range of 100–500 mK.

In conclusion, our analytical considerations and numerical simulations of a model Hamiltonian [1] of a disordered InAs wire on a superconducting substrate show three signatures of the transition into the topological phase (Figs. 1 and 2): A quantized thermal conductance and electrical shot noise [31], and a period doubling of the magnetoconductance oscillations. These unique signatures of the Majorana phase transition provide alternatives to the detection of Majorana bound states [9–13,15], which are fundamentally insensitive to the obscuring effects of disorder in a multimode wire.

We thank N. Read for alerting us to relevant literature. This research was supported by the Dutch Science Foundation NWO/FOM, by the Deutscher Akademischer Austausch Dienst DAAD, and by an ERC Advanced Investigator Grant.

[1] R. M. Lutchyn, J. D. Sau, and S. Das Sarma, Phys. Rev. Lett. **105**, 077001 (2010); Y. Oreg, G. Refael, and F. von Oppen, Phys. Rev. Lett. **105**, 177002 (2010).
[2] G. E. Volovik, JETP Lett. **66**, 522 (1997).
[3] N. Read and D. Green, Phys. Rev. B **61**, 10267 (2000).
[4] A. Yu. Kitaev, Phys. Usp. **44**, 131 (2001).
[5] F. Hassler, A. R. Akhmerov, C.-Y. Hou, and C. W. J. Beenakker, New J. Phys. **12**, 125002 (2010).
[6] J. Alicea, Y. Oreg, G. Refael, F. von Oppen, and M. P. A. Fisher, arXiv:1006.4395.
[7] J. D. Sau, S. Tewari, and S. Das Sarma, Phys. Rev. A **82**, 052322 (2010).
[8] J. A. van Dam, Y. V. Nazarov, E. P. A. M. Bakkers, S. De Franceschi, and L. P. Kouwenhoven, Nature (London) **442**, 667 (2006).
[9] K. T. Law, P. A. Lee, and T. K. Ng, Phys. Rev. Lett. **103**, 237001 (2009).
[10] J. Linder, Y. Tanaka, T. Yokoyama, A. Sudbø, and N. Nagaosa, Phys. Rev. Lett. **104**, 067001 (2010).
[11] H.-J. Kwon, K. Sengupta, and V. M. Yakovenko, Eur. Phys. J. B **37**, 349 (2004).
[12] L. Fu and C. L. Kane, Phys. Rev. B **79**, 161408(R) (2009).
[13] V. Shivamoggi, G. Refael, and J. E. Moore, Phys. Rev. B **82**, 041405 (2010).
[14] T. Neupert, S. Onoda, and A. Furusaki, Phys. Rev. Lett. **105**, 206404 (2010).
[15] K. Flensberg, Phys. Rev. B **82**, 180516 (2010).
[16] M. Z. Hasan and C. L. Kane, Rev. Mod. Phys. **82**, 3045 (2010); X.-L. Qi and S.-C. Zhang, arXiv:1008.2026.
[17] F. Merz and J. T. Chalker, Phys. Rev. B **65**, 054425 (2002).
[18] M. Bocquet, D. Serban, and M. Zirnbauer, Nucl. Phys. **B578**, 628 (2000).
[19] P. W. Brouwer, A. Furusaki, I. A. Gruzberg, and C. Mudry, Phys. Rev. Lett. **85**, 1064 (2000); P. W. Brouwer, A. Furusaki, and C. Mudry, Phys. Rev. B **67**, 014530 (2003).
[20] O. Motrunich, K. Damle, and D. A. Huse, Phys. Rev. B **63**, 224204 (2001).
[21] I. A. Gruzberg, N. Read, and S. Vishveshwara, Phys. Rev. B **71**, 245124 (2005).
[22] For a review of class-D ensembles of disordered superconducting wires we refer to Sec. 5.F of F. Evers and A. Mirlin, Rev. Mod. Phys. **80**, 1355 (2008).
[23] There exist, in addition to class D, four more symmetry classes with a topological phase transition in a wire geometry. As we will show elsewhere, the quantized conductance at the transition point appears generically. This is a manifestation of the "superuniversality" of Ref. [21].
[24] See supplemental material at http://link.aps.org/supplemental/10.1103/PhysRevLett.106.057001.
[25] We need an even number of modes to calculate Q without any sign ambiguity, so the single disordered mode described by the Hamiltonian (4) is supplemented by a second clean mode in a topologically trivial phase (uniform $\Delta_0 > 0$). The sign of Q is then completely determined by the sign of r in Eq. (6).
[26] M. Wimmer and K. Richter, J. Comput. Phys. **228**, 8548 (2009).
[27] M. Wimmer, A. R. Akhmerov, M. V. Medvedyeva, J. Tworzydło, and C. W. J. Beenakker, Phys. Rev. Lett. **105**, 046803 (2010).
[28] A. C. Potter and P. A. Lee, Phys. Rev. Lett. **105**, 227003 (2010).
[29] R. M. Lutchyn, T. Stanescu, and S. Das Sarma, arXiv:1008.0629.
[30] M. P. Anantram and S. Datta, Phys. Rev. B **53**, 16390 (1996).
[31] We do not plot the quantized shot noise peak in a separate figure, because our numerical simulation shows that P in units of $e^3V_1/2h$ is indistinguishable on the scale of Fig. 1 from G_{th} in units of G_0.
[32] M. Büttiker and T. M. Klapwijk, Phys. Rev. B **33**, 5114 (1986).
[33] C. Benjamin and J. K. Pachos, Phys. Rev. B **81**, 085101 (2010).